



# Structural fluctuations and role of Ti as nucleating agent in an aluminosilicate glass

Marie Guignard<sup>a</sup>, Laurent Cormier<sup>a,\*</sup>, Valérie Montouillout<sup>b,c</sup>, Nicolas Menguy<sup>a</sup>, Dominique Massiot<sup>b,c</sup>

<sup>a</sup> Institut de Minéralogie et de Physique des Milieux Condensés (IMPMC), Université Pierre et Marie Curie Paris 6, CNRS UMR 7590, Université Denis Diderot, IPGP, 140 rue de Lourmel, 75015 Paris, France

<sup>b</sup> Conditions Extrêmes et Matériaux, Haute Température et Irradiation (CEMHTI), CNRS UPR 3079, 1D avenue de la Recherche Scientifique, 45071 Orléans cedex 2, France

<sup>c</sup> Université d'Orléans, Faculté des Sciences, avenue du Parc Floral, BP 6749 45067 Orléans cedex 2, France

## ARTICLE INFO

### Article history:

Received 22 September 2009

Available online 17 May 2010

### Keywords:

Aluminosilicates A165;

Atomic structure A247;

Crystal nucleation C2865

## ABSTRACT

Nucleation is the initiating event for the formation of any crystal from undercooled melt. Although the classical nucleation theory describes qualitatively many aspects of the crystallization process, the mechanisms favoring the first steps of nucleation are still unknown and required the full identification of the catalytic sites. In this work, we report a structural investigation of the system  $2\text{MgO}-2\text{Al}_2\text{O}_3-5\text{SiO}_2 + \text{TiO}_2$ , a major glass-ceramic for scientific and industrial interest, in order to understand the structural influence of Ti as a nucleating agent. X-ray scattering and  $^{27}\text{Al}$  Nuclear Magnetic Resonance studies were carried out on  $2\text{MgO}-2\text{Al}_2\text{O}_3-5\text{SiO}_2 + x\text{TiO}_2$  glasses, with  $0 \text{ mol}\% \leq x \leq 15.5 \text{ mol}\%$ .

No evidence of phase separation can be detected in the initial glasses by Transmission Electron Microscopy at nanoscale and Ti atoms appear to be homogeneously distributed within the glassy structure. We explain that the presence of  $\text{TiO}_2$  favors nucleation by the formation in the initial glass of high-coordinated Al species and the presence of structural fluctuations that mimic the initial crystalline phase precipitating in the glass. The understanding of the parent glass structure appears as a critical constraint to understand the pathways promoting nucleation.

© 2010 Elsevier B.V. All rights reserved.

## 1. Introduction

Titanium is an important element in glass technology as one of the most efficient nucleating agent used for the fabrication of glass-ceramics [1]. These materials are most commonly made by forming glasses and then applying a controlled heat treatment to nucleate and precipitate crystals in the glassy matrix. Titanium acts as an efficient nucleant which promotes controlled bulk nucleation but the underlying mechanisms have not been entirely explained yet.

A nucleating agent can promote nucleation by accelerating phase separation or by lowering the energy barrier of nucleation. Upon the heat treatment that are used to obtained nucleation in the system  $\text{MgO}-\text{Al}_2\text{O}_3-\text{SiO}_2-\text{TiO}_2$ , the development of a micro-inhomogeneous structure with the decomposition to two amorphous states is often considered [2–10] and the terms phase separation or glass-in-glass separation are usually used.

The concept of phase separation was originally proposed by Maurer's work based on light scattering that showed the presence of small inhomogeneities in a titanium-bearing magnesium aluminosilicate glass even before the nucleation process [11]. This was interpreted by the presence of titanium-rich droplets and the formation of titanium-rich and silicon-rich regions was confirmed later for heat-treated glasses [6,12,13]. These regions can be the starting point for the internal

crystallization of the volume of the glass enabling, at higher temperatures, the nucleation of (Mg–Al)-titanate crystals before or simultaneously with a  $\beta$ -quartz solid solution [2–4,7,8,12,14–19]. This amorphous–amorphous phase separation appears almost simultaneously with the formation of the smallest crystals [13,20], which lead to difficulties to differentiate both processes.

It is still not clear if the phase separation observed after prolonged high-temperature annealing can reflect any phase separation in the initial glass. In all studies, the starting samples are X-ray amorphous glasses according to X-ray diffraction (XRD) data, but this method is not appropriate to distinguish glass-in-glass separation. Indisputably, small angle X-ray scattering (SAXS) and neutron scattering (SANS) are useful experimental tools to characterize structure heterogeneities in the size range between 1 nm and some hundreds of nm. In fact, past studies have shown contradictory results. No SANS signal was observed in as quenched glasses [6,13], even after heat treatment at 720 °C for 10 h [20] or at 750 °C for 30 h [6]. The absence of two amorphous structures in the initial glass was confirmed in several studies using transmission electron microscopy (TEM) [19,21,22]. On the contrary, using SAXS, two kinds of regions of inhomogeneity were identified in the initial glass, with significantly distinguished mean sizes of 2.0 and 6–40 nm in diameter [16,23]. The micro-inhomogeneous structure has been interpreted as a liquid–liquid phase separation that proceeds in the course of melt cooling.

$\text{TiO}_2$  has been used to catalyze heterogeneous nucleation in aluminosilicate glasses and its effect on their crystallization has been

\* Corresponding author.

E-mail address: [cormier@impmc.jussieu.fr](mailto:cormier@impmc.jussieu.fr) (L. Cormier).

intensively studied over the last 50 years [24]. However, the initial glass structure has been rarely characterized. Few investigation report the structural modifications that occur within the glass network with the addition of TiO<sub>2</sub> [25,26]. This lack of investigation explains why the Ti role in promoting devitrification and/or vitreous phase separation is still not clear. The experimental challenge is due to difficulties of gaining detailed structural information about the small composition fluctuations at the atomic scale from which the precipitate develops.

In this paper, we aim to study the structural modifications induced by the introduction of TiO<sub>2</sub> in MgO–Al<sub>2</sub>O<sub>3</sub>–SiO<sub>2</sub> glasses and to understand the role of titanium in promoting the devitrification process. We focused our work on the cordierite composition (2MgO–2Al<sub>2</sub>O<sub>3</sub>–5SiO<sub>2</sub>), in which titanium dioxide was gradually added. This system is of considerable technological importance and has been widely used to make quantitative tests of nucleation theories [27]. We have used experimental techniques sensitive to either the overall glass structure, X-ray scattering and TEM, or the local aluminum environment, <sup>27</sup>Al Nuclear Magnetic Resonance (NMR).

## 2. Experimental procedure

### 2.1. Preparation of glasses

Glasses with compositions 2MgO–2Al<sub>2</sub>O<sub>3</sub>–5SiO<sub>2</sub> + xTiO<sub>2</sub> with  $x = 0, 3.4, 7.1, 11.1$  and 15.5 mol%, were synthesized by melting the dried starting materials (MgO, Al<sub>2</sub>O<sub>3</sub>, SiO<sub>2</sub> and TiO<sub>2</sub>) 1 h at 1600 °C in a platinum crucible. Glasses were obtained by immersing the bottom of the crucible into water. The obtained glasses were ground and melt once again to ensure a good homogeneity.

### 2.2. Techniques of characterization

The compositions were determined using electron microprobe microanalyser (CAMECA SX50) at the Camparis Centre (Université Pierre et Marie Curie, France) with an accuracy of  $\pm 0.3$  mol%. The densities were determined in toluene using the Archimedes's principle with an accuracy of  $\pm 0.005$  g/cm<sup>3</sup>. The chemical compositions of the studied glasses are reported in Table 1, as well as their densities. After synthesis, the glass samples containing titanium are transparent, no sign of opalescence and exhibited a slight brownish color because of the reduction of some Ti<sup>4+</sup> ions into Ti<sup>3+</sup> ions. As trivalent titanium ions were the only ions with a free electron, we calculated their amount in the glass samples by using Electron Paramagnetic Resonance (EPR) (Bruker), indicating less than 300 ppm Ti<sup>3+</sup> ions of total titanium atoms.

Differential thermal analyses (DTA) were carried out on glass powder (~200 mg) in platinum crucible in the temperature range of 25 to 1500 °C. The measurements were performed at a heating rate of 10 °C/min. The onset glass transition temperatures were determined with an accuracy of  $\pm 2$  °C.

Transmission Electron Microscopy (TEM) observations were carried out on a JEOL 2100F microscope operating at 200 kV, equipped with a field emission gun, a high-resolution UHR pole piece and a Gatan US4000 CCD camera. Elemental mapping were performed using X-ray Energy Dispersive Spectroscopy (XEDS) analyses using a JEOL

detector coupled with a scanning TEM device. Using the three window technique [28], Energy Filtered TEM (EFTEM) was performed with a GATAN Imaging filter 2001.

The X-ray scattering experiment was carried out using a diffractometer (PANalytical X'Pert PRO) operating with a MoK $\alpha$  radiation ( $\lambda = 0.7093$  Å). Intensities were measured in the angular range  $2 < 2\theta < 148^\circ$ , which corresponds to the  $Q$ -range  $0.3 < 2\theta < 17$  Å<sup>-1</sup> ( $Q = 4\pi\sin\theta/\lambda$ ). Data were corrected for polarization and absorption, Compton scattering and normalized using the Krogh–Moe–Norman method [29] to obtain the weighted structure factor  $F(Q)$  defined as:

$$F(Q) = \sum_{ij} c_i c_j f_i(Q) f_j(Q) [F_{ij}(Q) - 1] / \left( \sum_i c_i f_i(Q) \right)^2 \quad (1)$$

where  $c_i$  is the atomic concentration,  $f_i(Q)$  is the  $Q$ -dependant X-ray scattering factor and  $F_{ij}(Q)$  is the partial structure factor corresponding to the correlation between atoms  $i$  and  $j$ . The differential correlation function  $D(r)$  is obtained by Fourier transform of the total structure factor, whose expression is:

$$D(r) = \frac{2}{\pi} \int_0^\infty Q F(Q) M(Q) \sin(Qr) dQ \quad (2)$$

where  $M(Q)$  is a modification function to limit the truncation effects. An exponential function,  $\exp(-\alpha Q^2)$  with  $\alpha = 0.005$ , is chosen as the modification function. Finally  $D(r)$  function is defined in term of the partial pair distribution functions (PPDFs),  $g_{ij}(r)$ , corresponding to the correlation between atoms  $i$  and  $j$ , convoluted with the Fourier transform of the X-ray scattering factors,  $f_i(Q)$ :

$$D(r) = 4\pi\rho_0 \left\{ \left[ r \left( g_{ij}(r) - 1 \right) \right] \otimes FT \left( f_{ij}(Q) \right) \right\} \quad (3)$$

where  $\rho_0$  is the number density and  $f_{ij}(Q) = f_i(Q)f_j(Q) / [\sum_i c_i f_i(Q)]$ .

The <sup>27</sup>Al NMR high-resolution NMR spectra have been obtained with a high field Bruker AVANCE spectrometer (17.6 T–750 MHz) equipped with high speed MAS probe heads (spinning rate of 30 kHz, aluminum free zirconia rotors of 2.5 mm diameter). The <sup>27</sup>Al 1D spectra have been acquired using a one pulse sequence. The pulse angle was small enough and the recycling delay (1 s) long enough to ensure quantitative interpretation. The Multiple Quantum Magic Angle Spinning (MQMAS [30]) experiments have been acquired using the shifted-echo pulse sequence with acquisition and processing of the full echo [31] and synchronized acquisition of the indirect dimension [32]. The triple quantum excitation and conversion were achieved under high power irradiation ( $\nu_{rf} \sim 150$  kHz) and the shifted-echo generation with low power pulse ( $\nu_{rf} \sim 12$  kHz).

## 3. Results

The chemical composition of the five studied glasses is reported in Table 1 with their atomic densities and their onset of glass transition temperatures ( $T_g$ ) determined by DTA. A monotone decrease of  $T_g$  is observed as the titanium content increases, from 802 °C for the Ti-free glass to 735 °C for the glass containing 15.5 mol% TiO<sub>2</sub>, respectively. This variation agrees with previous studies showing a decrease in  $T_g$  with the addition of TiO<sub>2</sub> [3,25,33].

The homogeneity of the two glasses containing the highest amount of TiO<sub>2</sub> ( $x = 11.1$  and 15.5 mol%) was characterized using TEM and bright field images recorded for the two samples are shown in Fig. 1. Both of these glasses are homogeneous and no evidence of phase separation is observed. The homogeneity of the sample has been also verified using chemical sensitive techniques (e.g. EFTEM and STEM high angle annular dark field imaging) and no chemical heterogeneities have been observed in the detection limits of our equipment, which is about 1 nm.

**Table 1**  
Chemical composition (mol%), density  $\rho$  (g cm<sup>-3</sup>) and glass transition temperature  $T_g$  (°C) for the glasses 2MgO–2Al<sub>2</sub>O<sub>3</sub>–5SiO<sub>2</sub> + x mol% TiO<sub>2</sub>.

	MgO	Al <sub>2</sub> O <sub>3</sub>	SiO <sub>2</sub>	TiO <sub>2</sub>	$\rho$	$T_g$
$x = 0$	21.6	22.7	55.8		2.62	802
$x = 3.4$	20.2	22.0	54.5	3.3	2.64	783
$x = 7.1$	21.9	20.6	50.9	6.6	2.66	765
$x = 11.1$	21.0	19.8	49.2	10.0	2.70	749
$x = 15.5$	20.1	19.1	47.2	13.6	2.74	735

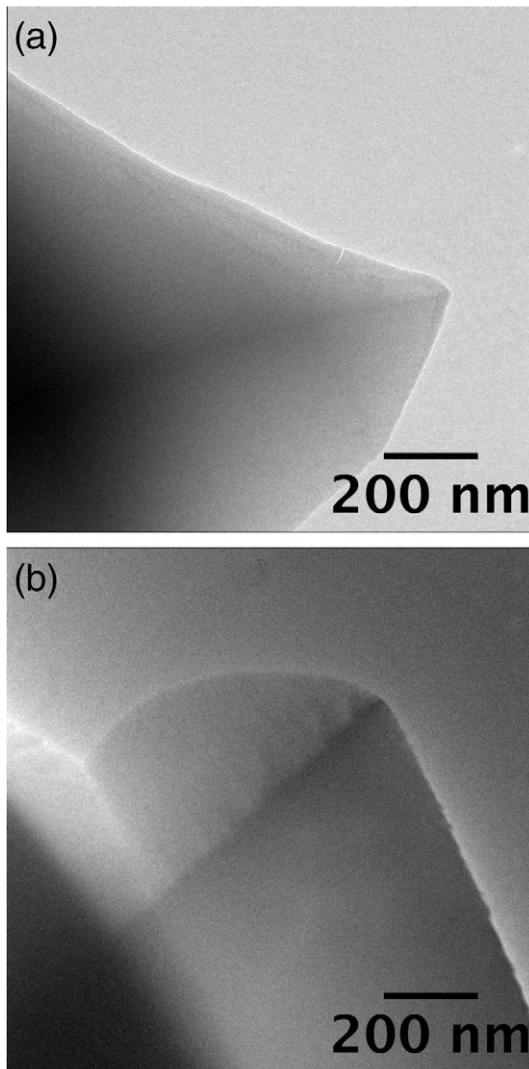


Fig. 1. Bright field TEM images for the glasses  $2\text{MgO}-2\text{Al}_2\text{O}_3-5\text{SiO}_2 + x \text{ mol\% TiO}_2$ , with (a)  $x = 11.1$  and (b)  $x = 15.5$ .

The weighted X-ray scattering structure factors  $F(Q)$  are plotted in Fig. 2. A first peak occurs at  $Q = 1.87 \pm 0.02 \text{ \AA}^{-1}$ , whose intensity is slightly higher in the case of the Ti-free glass. This peak is a signature of medium range order associated with density fluctuations. The differential correlation functions  $D(r)$  for the three glasses are shown in Fig. 3. For the Ti-free glass the first peak appears around  $1.7 \text{ \AA}$  and encompasses both Si–O and Al–O correlations. The shoulder observed at  $2.1 \text{ \AA}$  results from Mg–O correlations. The second peak centered at  $3.1 \text{ \AA}$  is due to the overlap of two contributions: the O–O correlations that generate a shoulder at  $2.6 \text{ \AA}$  and the T–T correlations that largely dominate around  $3.1 \text{ \AA}$ , with  $T = \text{Si}$  or Al. This latter peak is associated mainly with Si and Al because of the smaller atomic content of Mg (6.9 at.%) compared to Si (17.2 at.%) and Al (13.8 at.%). Finally the third peak at  $4.2 \text{ \AA}$  is mainly due to the correlations between (Si, Al) and O second neighbors. With the addition of  $\text{TiO}_2$ , the intensity of the first peak decreases as both Si and Al contents decrease. In the same time, two new contributions appear on the  $D(r)$  functions. The first one, centered at  $1.9 \text{ \AA}$ , is assigned to the Ti–O correlations, and the second one, observed around  $3.3 \text{ \AA}$ , can be attributed to Ti–T correlations, with  $T = \text{Si, Al, Mg}$  or Ti.

$^{27}\text{Al}$  1D and 2D-NMR spectra for the five glasses are presented in Fig. 4. In all of them, the main signal is unambiguously assigned to aluminum four-fold coordinated to oxygen,  $^{[4]}\text{Al}$ . Furthermore, the

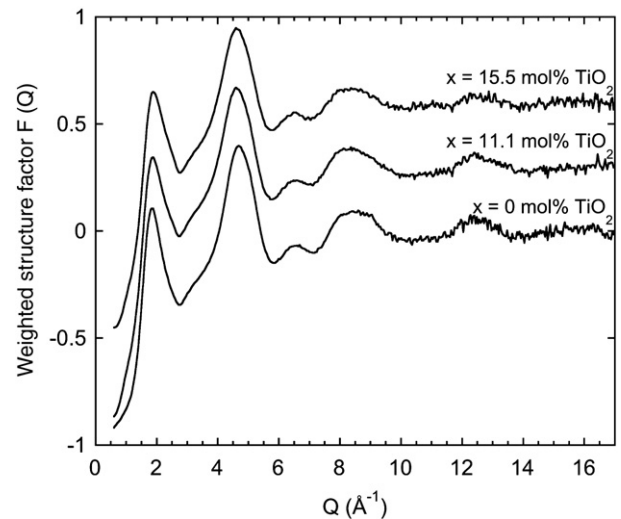


Fig. 2. Weighted X-ray scattering structure factor  $F(Q)$  obtained from the X-ray diffraction for the glasses  $2\text{MgO}-2\text{Al}_2\text{O}_3-5\text{SiO}_2 + x \text{ mol\% TiO}_2$ , with  $x = 0, 11.1$  and  $15.5 \text{ mol\%}$ .

spectra also show the presence of highly coordinated aluminum atoms, i.e. aluminum atoms with five ( $^{[5]}\text{Al}$ ) or six ( $^{[6]}\text{Al}$ ) oxygen neighbors. The 2D spectra were deconvoluted using the “dmfit” program [34] to retrieve the isotropic chemical shift,  $\delta_{\text{iso}}$ , and the mean quadrupolar product,  $C_{\text{QI}}$ , for each aluminum species. These parameters were then used to simulate the 1D quantitative MAS spectra and estimate the amount of  $^{[4]}\text{Al}$ ,  $^{[5]}\text{Al}$  and  $^{[6]}\text{Al}$  as described earlier [35]. Values are reported in Table 2; error bars are  $\pm 0.5 \text{ ppm}$  for the  $\delta_{\text{iso}}$  and about  $\pm 0.5 \text{ MHz}$  for the  $C_{\text{QI}}$ , and the uncertainties on the proportion of five-fold coordinated,  $^{[5]}\text{Al}$ , and six-fold coordinated,  $^{[6]}\text{Al}$ , aluminum are around 1% [34]. No significant variations of chemical shift or quadrupolar coupling constant can be observed with the titanium content. Moreover, we observe that the amount of highly coordinated aluminum atoms increases gradually with increasing  $\text{TiO}_2$  content and reaches more than one fifth of the total number of aluminum atoms for the glass with the highest Ti content.

#### 4. Discussion

The  $2\text{MgO}-2\text{Al}_2\text{O}_3-5\text{SiO}_2$  cordierite glass corresponds to tectosilicate compositions for which, based on the stoichiometric formula, no

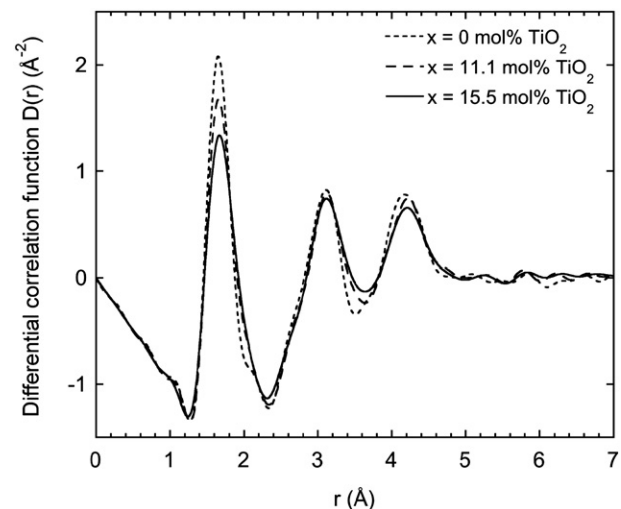
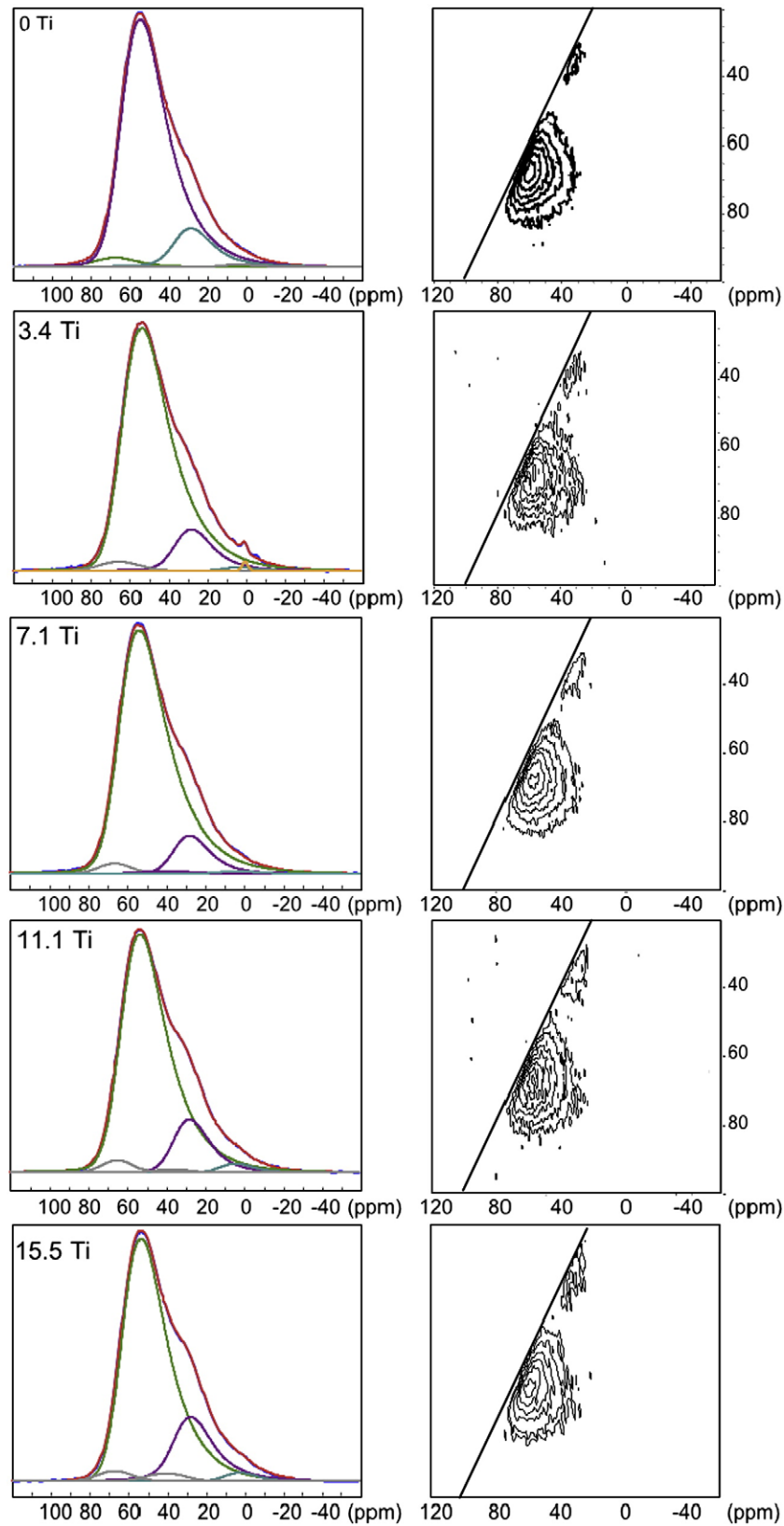


Fig. 3. Differential correlation function  $D(r)$  obtained from the X-ray diffraction for the glasses  $2\text{MgO}-2\text{Al}_2\text{O}_3-5\text{SiO}_2 + x \text{ mol\% TiO}_2$ , with  $x = 0, 11.1$  and  $15.5 \text{ mol\%}$ .



**Fig. 4.** The left column represents the 1D  $^{27}\text{Al}$  NMR experimental spectra and the fitting models obtained with parameters that are given in Table 1, for the glasses containing 0 mol%  $\text{TiO}_2$  (top) to the glass containing 15.5 mol%  $\text{TiO}_2$  (bottom). The right column is the corresponding contour plots of  $^{27}\text{Al}$  MQ-MAS NMR. The plain line represents chemical shift axis. A small crystalline peak is seen in the sample with 3.4 mol%  $\text{TiO}_2$  though no Bragg peaks can be detected with X-ray diffraction.

non-bridging oxygen atoms (NBO) or highly coordinated aluminum atoms are expected. This statement has been found to be erroneous in recent years by the use of  $^{17}\text{O}$  [36] and  $^{27}\text{Al}$  NMR [37–39] that showed

the presence of NBOs or highly coordinated aluminum atoms for tectosilicate glasses in alkaline-earth aluminosilicate systems. It was demonstrated that the amount of highly coordinated aluminum

**Table 2**

$^{27}\text{Al}$  NMR parameters of the different aluminum species, extracted from the fitting models of 1D MAS spectra.  $\delta_{\text{iso}}$  is the isotropic chemical shift (ppm),  $\text{CQ}_{\text{T}}$  is the mean quadrupolar product (MHz).

	$^{[4]}\text{Al}$			$^{[5]}\text{Al}$			$^{[6]}\text{Al}$		
	$\delta_{\text{iso}}$	CQ	%	$\delta_{\text{iso}}$	CQ	%	$\delta_{\text{iso}}$	CQ	%
$x=0$	63.6	8.54	87.0	35.0	6.99	12.4	10.0	6.11	0.6
$x=3.4$	63.6	8.97	87.0*	35.0	6.99	12.2*	10.0	6.10	0.8*
$x=7.1$	63.6	8.90	89.0	35.0	6.99	10.4	10.0	6.10	0.6
$x=11.1$	63.6	8.52	83.3	34.3	6.99	14.6	10.0	6.10	2.1
$x=15.5$	63.7	8.52	78.3	34.3	6.99	19.9	8.7	6.10	1.8

\* Relative quantification of  $^{[4]}\text{Al}$ ,  $^{[5]}\text{Al}$  and  $^{[6]}\text{Al}$ , regardless of any crystalline impurities.

atoms increases when cation field strength increases ( $\text{Mg}^{2+} > \text{Ca}^{2+}$ ) and that it could reach up to 15% of the total number of aluminum atoms in the tectosilicate glass  $\text{MgO}-\text{Al}_2\text{O}_3-2\text{SiO}_2$  [38]. The present results on the Ti-free cordierite glass confirm the presence of both  $^{[5]}\text{Al}$  and  $^{[6]}\text{Al}$  species. Further information about the structure and the local environment of silicon and magnesium atoms in the tectosilicate glass has been reported in a previous paper [40].

With the addition of titanium oxide, the glass remains chemically homogeneous even at the highest amount of  $\text{TiO}_2$  ( $x=11.1$  and 15.5 mol%) as revealed by TEM and bright field images (Fig. 1). This indicates that titanium atoms are homogeneously distributed within the aluminosilicate network. Up to now it has been supposed that the nucleation is a kinetically complex process driven initially by an amorphous phase separation which enables the subsequent formation of crystalline nuclei. It has been suggested that  $\text{TiO}_2$  in glasses may operate as surface-active agents, shift the immiscibility boundary, or affect the kinetics of phase separation [2,41]. If phase separation is favored, we could expect that increasing the Ti content will promote such behavior, which is not experimentally observed using TEM (Fig. 1). The lack of phase separation in the parent glasses agrees with a recent high-resolution TEM investigation [19]. In this study, it was proposed that the formation of crystallites proceeds by re-arrangement and successive displacement of the local ordering of atoms within the glass structure. In such a mechanism, glass-in-glass separation is not necessary for the onset of glass crystallization.

Unmixing phenomenon is established in the  $\text{TiO}_2-\text{SiO}_2$  binary system [42]. However it is not obvious that similar immiscibility exists in Ti-bearing complex glasses. For example  $\text{Al}_2\text{O}_3-\text{SiO}_2$  binary system is also known to exhibit liquid-liquid immiscibility [43], but complex alkaline-earth aluminosilicate glasses have a homogeneous structure and an almost random substitution of Si by Al in tetrahedral sites [44]. We can thus conclude that titanium is homogeneously distributed in the Ti-bearing glasses investigated in this paper. In our study, no evidence for phase separation or strongly inhomogeneous density or chemical distribution can be observed, implying that if phase separation occurs, it is a thermally activated process.

The X-ray scattering data show that the addition of  $\text{TiO}_2$  does not strongly modify the structure, even with addition of up to 15.5 mol%  $\text{TiO}_2$ . Similar results are also observed using neutron diffraction [45]. The correlations between the main atomic pairs (Si-O, Al-O, Si-Si/Al...) occur at similar distances in Ti-bearing glasses than in the Ti-free glass. Our structural characterization thus indicates that the main structural modifications induced by the addition of titanium in magnesium aluminosilicate glasses is the enhancement of the amount of highly coordinated aluminum atoms, observed by solid state  $^{27}\text{Al}$  NMR.

We have previously shown that highly coordinated aluminum atoms tend to segregate to form clusters of about three or four  $\text{AlO}_5$  entities in  $\text{MgO}-\text{Al}_2\text{O}_3-\text{SiO}_2$  glasses [40]. More recently, we reported the tendency for titanium atoms to bond with highly coordinated aluminum atoms by edge-sharing in the  $2\text{MgO}-2\text{Al}_2\text{O}_3-5\text{SiO}_2 +$

11.1 mol%  $\text{TiO}_2$  glass [45]. Such an arrangement extracted from a Reverse Monte Carlo modeling is represented in Fig. 5. We demonstrate here that the amount of highly coordinated aluminum atoms in magnesium aluminosilicate glasses increases as  $\text{TiO}_2$  content increases. Ti could increase distortion of the network, or non-random distribution of the elements. Since both  $^{[5]}\text{Ti}$  and Al require charge-compensation by alkaline-earths, their association optimizes the double charge of  $\text{Mg}^{2+}$  ions. A similar behavior is seen in aluminosilicate glasses, with the formation of Al-O-Al linkages increasing with the cation field strength [46].

In the  $\text{MgO}-\text{Al}_2\text{O}_3-\text{SiO}_2-\text{TiO}_2$  glass system, nucleation begins with the formation of a phase in low concentration corresponding to a magnesium aluminotitanate in the  $\text{MgTi}_2\text{O}_5-\text{Al}_2\text{TiO}_5$  solid solution [2-4,7,8,12,14-19]. We have shown that the molar composition of the nano-crystals is close to  $(\text{MgTi}_2\text{O}_5)_{40}-(\text{Al}_2\text{TiO}_5)_{60}$  [47]. These phases are built from edge-shared  $\text{MgO}_6$ ,  $\text{AlO}_6$  and  $\text{TiO}_6$  octahedra [48,49]. The structural arrangement in Fig. 5 shows important similarities with the crystalline ordering. We can thus conclude that the catalytic effect of titanium on the nucleation of aluminosilicate lies in the existence of preferential edge-sharing linkage between titanium atoms and highly coordinated aluminum atoms, whose amount is expected to increase when  $\text{TiO}_2$  content increases. This structural fluctuations preexisting in the glass can be considered as the seeds for the formation of critical nuclei. These complexes involve few polyhedra so that the density or composition fluctuations are likely too small to be detected by techniques such as SAXS or SANS. These complexes will first favor the formation of titanate phases since small atomic diffusion will be required and the thermodynamic barrier to the formation of a nucleus will be easily overcome. Enough activation energy for diffusion will be available at high undercooling close to the glass transition temperature allowing small structural rearrangements.

Our results agree with theoretical studies showing that local favorable inhomogeneities in randomly disordered media such as glasses may reduce the height of the thermodynamic nucleation barrier and increase its temperature dependence [50]. These effects

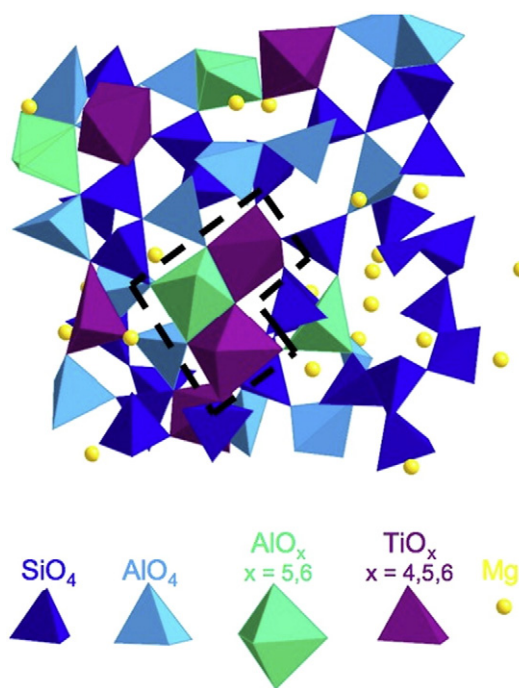


Fig. 5. Detail of the structure of the glass  $2\text{MgO}-2\text{Al}_2\text{O}_3-5\text{SiO}_2 + 11.1 \text{ mol\% TiO}_2$  obtained from RMC modeling (Details of the procedure of the RMC modeling are given in Ref. [45]).

may at least partly account for the discrepancy between theory and experiment in the Classical Nucleation Theory (CNT) [27,51,52] by increasing the nucleation rates exponentially [50]. CNT requires a source of heterophase fluctuations, without any precise definition. The static structural fluctuations evidenced in this study can be critical fluctuations that can rearrange to adopt a crystalline order or that can grow further to produce the amorphous–amorphous separation with regions enriched in the magnesium, aluminum and titanium oxides from which the magnesium aluminotitanate phase can precipitate. Clearly, the knowledge of the precise glass structure is important to understand these critical metastable fluctuations that allow the system to surmount the thermodynamic barrier between the glassy and crystalline phases.

Nucleation process requires bondbreaking and re-arrangement of the structure. However at high undercooling (near  $T_g$ ), the atomic mobility must remain limited so that primary nano-crystals should have a structure and composition close to that of the initial glass [19]. It can also be proposed that the mobility at the atomic scale is achieved by lowering the viscosity. Indeed, addition of  $\text{TiO}_2$  causes a reduction in  $T_g$  values (Table 1) which could lead to the formation of domains with a low viscosity promoting crystallization.

Another important result of this study is the dependence of the proportion of high-coordinated Al species with the  $\text{TiO}_2$  content. The amount of high-coordinated Al is between 11 and 13% for  $\text{TiO}_2$ –7.1 mol% and then increases to 16.7% for 11.1 mol%  $\text{TiO}_2$  and 21.7% for 15.5 mol%  $\text{TiO}_2$ . There is thus a structural transition above 7.1 mol%  $\text{TiO}_2$  content, with an important increase in the proportion of  $^{[5]}Al$  and  $^{[6]}Al$ . It is also established that volume nucleation is most easily achieved with additions of  $\text{TiO}_2$  in excess of approximately 7 mol% [4]. This value is close to that where incubation time of nucleation disappears, at 9.2–10.9 mol%  $\text{TiO}_2$  [6]. We thus evidence a similar transition at 7 mol%  $\text{TiO}_2$  with an increase in the high-coordinated Al content and an increase of the volume nucleation. A straightforward explanation is an increase in structural fluctuations illustrated in Fig. 5 because more high-coordinated Al are formed with the addition of  $\text{TiO}_2$ . It is still not clear why an important change appear around 7 mol%. However, we can note that spectroscopic studies have shown that  $^{[4]}Ti$  sites are more present at low  $\text{TiO}_2$  content in silicate glasses [26,53,54]. A coordination change from  $^{[4]}Ti$  at dilute  $\text{TiO}_2$  concentration to  $^{[5]}Ti$  at higher concentration could be an explanation for the structural changes above 7 mol%  $\text{TiO}_2$ , but further investigation are required.

## 5. Conclusion

Our multitechnique approach has shown that the main influence of  $\text{TiO}_2$  addition on the glass structure is the formation of five- and six-fold coordinated aluminum species. These high-coordinated species can form edge-shared linkages with Ti polyhedra, forming structural fluctuations bearing similarities with the first crystalline phases precipitating upon heat treatment. Thereby, the capacity of Ti to control nucleation depends on the medium range organization of the parent glass with structural fluctuations corresponding to precursors for critical nuclei. The  $\text{TiO}_2$  content is important since addition of  $\text{TiO}_2$  increases the amount of high-coordinated aluminum and thus the amount of critical fluctuations. These results provide the first experimental evidence of favorable structural organization that can be catalytic seeds for promoting nucleation. We can also emphasize the importance to have detailed structural information of the initial glass at atom-level details to unravel the origin of nucleation in disordered materials.

## Acknowledgments

We acknowledge O. Majérus and L. Michely from the Laboratoire de Chimie de la Matière Condensée de Paris for the thermal analyses. We thank Georges Calas for fruitful discussions. We would like also to thank the funding support by the French National Research Agency (ANR) under contract no. 06-JCJC-0010 “Nuclevitro”.

## References

- [1] P.W. McMillan, *Glass–Ceramics*, Academic Press, London and New York, 1979.
- [2] T.I. Barry, J.M. Cox, R.J. Morrell, *Mater. Sci.* 13 (1978) 594.
- [3] R.C. de Vekey, A.J. Maumdar, *Phys. Chem. Glasses* 16 (1975) 36.
- [4] V.M. Fokin, E.D. Zanotto, *J. Non-Cryst. Solids* 246 (1999) 115.
- [5] W. Höland, V. Rheinberger, M. Schweiger, *Phil. Trans. R. Soc. Lond. A* 361 (2003) 575.
- [6] A.A. Loshmanov, N. Sigaev, R.Y. Khodakovskaya, N.M. Pavlushkin, I.I. Yamzin, *J. App. Cryst.* 7 (1974) 207.
- [7] L.R. Pinckney, G.H. Beal, *J. Non-Cryst. Solids* 219 (1997) 219.
- [8] H. Shao, K. Liang, F. Peng, *Ceram. Inter.* 30 (2004) 927.
- [9] W. Zdaniewski, *J. Am. Ceram. Soc.* 61 (1978) 199.
- [10] X. Zou, M. Yamane, J. Li, C. Wang, *J. Non-Cryst. Solids* 112 (1989) 268.
- [11] R.D. Maurer, *J. Appl. Phys.* 33 (1962) 2132.
- [12] U. Lembke, R. Brückner, R. Kranold, Th. Höche, *J. Appl. Cryst.* 30 (1997) 1056.
- [13] A.F. Wright, A.N. Fitch, J.B. Hayter, B.E.F. Fender, *Phys. Chem. Glasses* 26 (1985) 113.
- [14] J. Dutkiewicz, L. Stoch, J. Morgiel, G. Kostorz, P. Stoch, *Mater. Chem. Phys.* 81 (2003) 41.
- [15] K. Furic, L. Stoch, J. Dutkiewicz, *Spectrochim. Acta A* 61 (2005) 1653.
- [16] V.V. Golubkov, O.S. Dymshits, A.A. Zhilin, T.I. Chuvaeva, A.V. Shashkin, *Glass Phys. Chem.* 29 (2003) 254.
- [17] S. Kumar, B.B. Nag, *J. Am. Ceram. Soc.* 49 (1966) 10.
- [18] K.-H. Park, D.-W. Shin, *J. Ceram. Proc. Res.* 3 (2002) 153.
- [19] L. Stoch, *Phys. Chem. Glasses: Eur. J. Glass Sc. Technol. B* 49 (2008) 183.
- [20] A.F. Wright, J. Talbot, B.E.F. Fender, *Nature* 277 (1979) 366.
- [21] F. Dumas, A. Ramos, M. Gandais, J. Petiau, *J. Mater. Sci. Lett.* 4 (1985) 129.
- [22] W. Zdaniewski, *J. Mater. Sci.* 8 (1973) 192.
- [23] T.I. Chuvaeva, O.S. Dymshits, P.I. Petrov, M.Y. Tsenter, A.V. Shashkin, A.A. Zhilin, V.V. Golubkov, *J. Non-Cryst. Solids* 282 (2001) 306.
- [24] S.D. Stookey, US patent (1960) US2.
- [25] R.-G. Duan, K.-M. Liang, S.-R. Gu, *Mater. Sci. Eng. A* 249 (1998) 217.
- [26] C. Romano, E. Paris, B.T. Poe, G. Giuli, D.B. Dingwell, A. Mottana, *Amer. Mineral.* 85 (2000) 108.
- [27] E.D. Zanotto, V.M. Fokin, *Phil. Trans. R. Soc. Lond. A* 361 (2003) 591.
- [28] M.K. Kundmann, O.L. Krivanek, *Micros. Microanal. Microstr.* 2 (1991) 257.
- [29] F. Marumo, M. Okuno, in: I. Sunagawa (Ed.), *Materials Science of the Earth's Interior*, Terra Scientific, Tokyo, 1984.
- [30] A. Medek, J.S. Harwood, L. Frydman, *J. Amer. Chem. Soc.* 117 (1995) 12779.
- [31] D. Massiot, B. Touzo, D. Trumeau, J.-P. Coutures, J. Virlet, P. Florian, P.J. Grandinetti, *Sol. St. Nucl. Mag. Res.* 6 (1996) 73.
- [32] D. Massiot, *J. Magn. Res. Ser. A* 122 (1996) 240.
- [33] D.T. Weaver, D.C. Van Aken, J.D. Smith, *J. Mater. Sci.* 39 (2004) 51.
- [34] D. Massiot, F. Fayon, M. Capron, I. King, S. Le Calve, B. Alonso, J.O. Durand, B. Bujoli, Z.H. Gan, G. Hoatson, *Mag. Res. Chem.* 40 (2002) 70.
- [35] D.R. Neuville, L. Cormier, D. Massiot, *Geochim. Cosmochim. Acta* 68 (2004) 5071.
- [36] J.F. Stebbins, Z. Xu, *Nature* 389 (1997) 60.
- [37] M.J. Toplis, S.C. Kohn, M.E. Smith, I.J.F. Poplett, *Amer. Mineral.* 85 (2000) 1556.
- [38] D.R. Neuville, L. Cormier, V. Montouillout, P. Florian, F. Millot, J.-C. Rifflet, D. Massiot, *Amer. Mineral.* 93 (2008) 1721.
- [39] D.R. Neuville, L. Cormier, V. Montouillout, D. Massiot, *J. Non-Cryst. Solids* 353 (2007) 180.
- [40] M. Guignard, L. Cormier, *Chem. Geol.* 256 (2008) 111.
- [41] W. Zdaniewski, *J. Amer. Ceram. Soc.* 58 (1975) 163.
- [42] P. Schultz, *J. Amer. Ceram. Soc.* 59 (1976) 214.
- [43] J.F. MacDowell, G.H. Beall, *J. Amer. Ceram. Soc.* 52 (1969) 17.
- [44] S.K. Lee, J.F. Stebbins, *J. Non-Cryst. Solids* 270 (2000) 260.
- [45] M. Guignard, L. Cormier, V. Montouillout, N. Menguy, D. Massiot, A.C. Hannon, *J. Phys.: Condens. Matter* 21 (2009) 375107.
- [46] S.K. Lee, G.D. Cody, B.O. Mysen, *Am. Mineral.* 90 (2005) 1393.
- [47] M. Guignard, L. Cormier, V. Montouillout, N. Menguy, D. Massiot, A.C. Hannon, B. Beuneu, *J. Phys.: Condens. Matter* 22 (2010) 185401.
- [48] H. Yang, R.M. Hazen, *J. Solid St. Chem.* 138 (1998) 238.
- [49] S.T. Norberg, N. Ishizawa, S. Hoffmann, M. Yoshimura, *Acta Crystallogr. A* E61 (2005) i160.
- [50] V.G. Karpov, D.W. Oxtoby, *Phys. Rev. B* 54 (1996) 9734.
- [51] J.W. Schmelzer, *J. Non-Cryst. Solids* 354 (2008) 269.
- [52] S. Sen, T. Mukerji, *J. Non-Cryst. Solids* 246 (1999) 229.
- [53] F. Farges, G.E. Brown Jr., A. Navrotsky, H. Gan, J.J. Rehr, *Geochim. Cosmochim. Acta* 60 (1996) 3039.
- [54] G.S. Henderson, X. Liu, M.E. Fleet, *Phys. Chem. Miner.* 29 (2002) 32.